Depth-resolved residual strain in MoN/Mo nanocrystalline films

Gang Chen,[a] Dileep Singh, Osman Eryilmaz, and Jules Routbort
Energy Technology Division, Argonne National Laboratory, Argonne, Illinois 60439

Bennett C. Larson
Materials Science and Technology Division, Oak Ridge National Laboratory, Oak Ridge, Tennessee 37831

Wenjun Liu
Advanced Photon Source, Argonne National Laboratory, Argonne, Illinois 60439

(Received 26 July 2006; accepted 7 September 2006; published online 23 October 2006)

The authors have applied cross-sectional x-ray microdiffraction to measure depth-resolved in-plane residual strain in nanocrystalline MoN/Mo bilayer films deposited on Si. Compressive strains with large gradients were found in the as-deposited films. After thermal annealing, the strain profiles and diffraction peak widths of the MoN and Mo layers were altered. These findings provide insights on the relationship between defects introduced during film processing and the effect of annealing on the structure and properties of magnetron-sputtered nanocrystalline films. © *2006 American Institute of Physics*. [DOI: 10.1063/1.2364131]

Thin films and coatings are widely used to reduce friction and to protect bulk materials from abrasion, corrosion, oxidation, and thermal shock. They have many applications in cutting tools, medical implants, microelectromechanical devices, tribological components, etc.[1] The coating performance is related to the adhesion between layer and substrate, which is strongly affected by residual stresses. Accordingly, understanding residual stresses and their spatial distribution in thin films is important for the development of reliable coatings with tailored properties.

Most stress analyses of thin films are based on the traditional $d-\sin^2\psi$ x-ray diffraction method or optical substrate curvature methods,[2] in which average stresses are measured over the x-ray or optical photon interaction volume.[3,4] Very few techniques can measure stress/strain gradients as a function of depth inside thin films and coatings. One such depth-resolved technique is based on the $d-\sin^2\psi$ method, in which the x-ray penetration depth into thin films is varied.[5,6] In the present study, we used cross-sectional x-ray microdiffraction to measure depth-resolved strain profiles in nanocrystalline MoN/Mo films with submicron resolution. By collecting x-ray diffraction patterns from different depths of the film, we obtained profiles of in-plane residual strain and diffraction peak width as a function of film depth. Compared to the other depth-resolved methods for studying thin films, this method is simpler and faster and provides more information.

MoN/Mo bilayer films were prepared by physical vapor deposition (PVD) using magnetron sputtering. A 99.5% pure molybdenum plate was used as the sputtering target. The substrate was a *p*-type single-crystal silicon wafer (100) (cleaved into $3\times3\times0.1$ cm^3 pieces) with a native oxide layer. The substrates were rotated and heated during deposition with an estimated temperature between 250 and 300 °C. A Mo bond layer was first deposited on the Si substrate, followed by deposition of a MoN layer. After deposition, some of the films were annealed at 500 °C in vacuum for 1 h. The as-deposited and annealed films were fractured along Si {110} planes to create smooth cross sections. Figure 1 is a scanning electron microscopy (SEM) micrograph of the cross section of an as-deposited MoN/Mo film. The Mo and MoN layers show a dense columnar structure.

X-ray microdiffraction was performed on beamline 34-ID-E at the Advanced Photon Source (Argonne National Laboratory).[7] The x-ray beam was focused by Kirkpatrick-Baez mirrors down to 0.4(horizontal)$\times$0.6(vertical) μm^2. The angle between the x-ray beam and the sample cross-section plane was 45°. A high-resolution charged coupled device x-ray detector was placed 30 mm above the sample to collect x-ray diffraction (XRD) patterns from the x-ray microbeam with an energy of 8.9 keV (1.393 08 Å). Before the XRD patterns were taken, the sample was aligned by an x-ray fluorescence method so that the film surface (i.e., the *yz* plane in Fig. 1) was parallel to the x-ray beam. The position of the x-ray beam was scanned along the film normal (*x* in Fig. 1) direction with a step size of 0.25 μm. Figures 2(a) and 2(b) show typical polycrystalline XRD patterns from the MoN and the Mo layers, respectively. The MoN film is a hexagonal phase with fiber texture such that the *c* axis is parallel to the film surface. The Mo film is a cubic phase with ⟨110⟩ fiber texture. Some of the films were scraped off the Si substrate using a diamond scriber and ground into a powder for determination of the strain-free lattice parameter. For the as-deposited and annealed hexagonal MoN, the measured strain-free lattice parameters are a=5.763 Å and c=5.6242 Å and a=5.7268 Å and c=5.6204 Å, respectively. For the as-deposited and annealed cubic Mo, the parameters

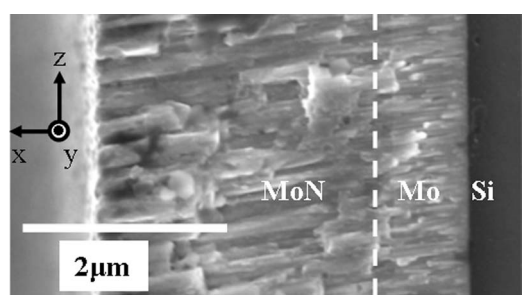

FIG. 1. Cross-sectional scanning electron micrograph of a MoN/Mo bilayer film deposited on a Si substrate.

[a]Electronic mail: gchen@anl.gov

 © 2006 American Institute of Physics
Downloaded 06 Sep 2009 to 160.91.157.167. Redistribution subject to AIP license or copyright; see http://apl.aip.org/apl/copyright.jsp

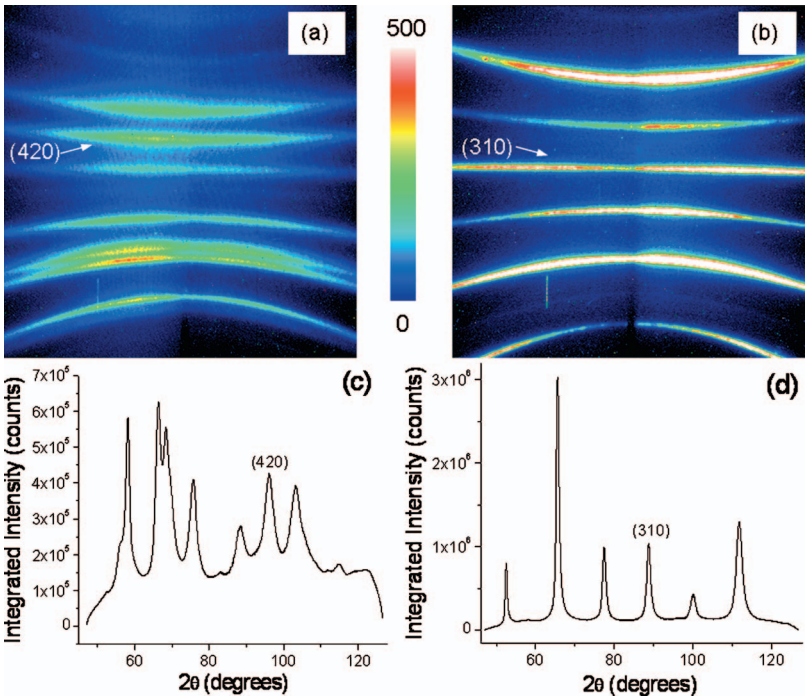

FIG. 2. (Color) Two-dimensional x-ray diffraction patterns of the MoN layer (a) and the Mo layer (b); (c) and (d) are integrated 1D patterns from (a) and (b), respectively.

are $a=3.1516$ Å and $a=3.1549$ Å, respectively. Figures 2(c) and 2(d) are the one-dimensional (1D) patterns of MoN and Mo derived from the two-dimensional patterns shown in Figs. 2(a) and 2(b), respectively. The (420) peak of MoN and (310) peak of Mo were selected for data analysis to have scattering vectors close to the normal of the cross-sectional plane (i.e., y in Fig. 1). Assuming isotropy in the plane of the film, this approach measures the in-plane lattice parameters, from which the in-plane strain can be determined. The XRD peaks were fitted by using an asymmetric pseudo-Voigt function, and the strain and the full width at half maximum (FWHM) of the diffraction peaks were derived as a function of depth from the film surface. Using the Scherrer formula,[8] the average grain sizes for the MoN and Mo layers were found to be 5 and 20 nm, respectively. The cross-sectional point-by-point scanning was repeated at different x positions along the sample to determine the variation of measured strain along the x direction.

Figure 3(a) shows depth-resolved in-plane strain (ε_y) profiles for the as-deposited and annealed MoN/Mo films. The thicknesses of the MoN and Mo layers were 2.7 and 0.8 μm, respectively. For the as-deposited film, the MoN layer was under in-plane compression, and the magnitude of the in-plane strain (ε_y) increased almost linearly with the depth. The maximum strain reached 0.005 at the MoN/Mo interface. The Mo layer was found to be under in-plane compression also, but the strain magnitude decreased with increasing depth. The maximum strain of 0.003 in the Mo layer appeared at the MoN/Mo interface.

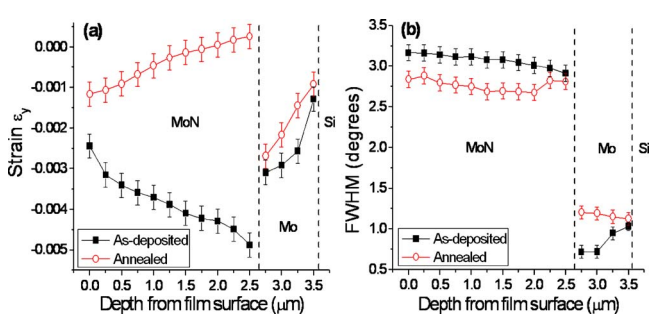

FIG. 3. (Color online) Depth-resolved residual strain (a) and FWHM (b) for as-deposited and annealed MoN/Mo bilayer films.

After annealing, the strain in the Mo film changed little and was still under in-plane compression. However, for the MoN layer, the overall strain magnitude decreased dramatically. The strain had its maximum of 0.0012 at the MoN surface and decreased linearly to essentially zero at the MoN/Mo interface. Figure 3(b) is a plot of the FWHM as a function of depth for both as-deposited and annealed films. For the as-deposited film, the FWHM of the MoN layer varied little with depth, while the diffraction width of the Mo layer increased with increasing depth. The FHWM of the MoN layer decreased slightly with annealing, but it was still relatively constant as a function of depth. For the Mo layer, the FWHM increased near the MoN/Mo interface, but there was almost no change near the Mo/Si interface.

Residual strains in PVD coatings are very complex because they include both intrinsic and extrinsic strains.[9] The intrinsic strains are related to the microstructure of thin films, which varies with material as well as with film deposition conditions. Extrinsic effects here refer to thermal strain caused by the thermal expansion coefficient mismatch between film and substrate. The differential thermal strain in the Mo and MoN layers of as-deposited and annealed films was estimated to be less than 10^{-3}; this value is much smaller than the residual strains observed in the films and will be neglected in further discussion.

In PVD films, the intrinsic residual strain is strongly affected by deposition conditions and is very difficult to model. Nonetheless, it is believed that compressive strains in thin films that have been subjected to ion or atom bombardment are caused by atomic peening,[10] which is enhanced by low sputtering gas pressure and high substrate bias during deposition.[9] The strain profile observed in the Mo layer is similar to the near-surface strain profiles in shot-peened bulk metals,[11] i.e., both have high compressive strain near the

Downloaded 06 Sep 2009 to 160.91.157.167. Redistribution subject to AIP license or copyright; see http://apl.aip.org/apl/copyright.jsp

surface, and the magnitude of strain decreases as the depth increases. Since strain profiles in PVD films may be complicated by defects, voids, trapped gas ions, impurities, and dislocations introduced during film deposition,[9] there should be differences between these two peening processes. However, the similarity in strain profiles suggests that the bombardment of the film by atoms/ions during its growth may be partially responsible for the observed strain profile in the Mo layer. The case of the MoN layer is more complicated since N_2 was introduced during the film growth to form the metal nitride. The maximum residual strain in the MoN layer is at the MoN/Mo interface, decreasing sharply as the film surface is approached. It is possible that the decrease is the result of a relaxation process during growth. As shown in Fig. 1, the Mo layer has a dense columnar structure, and the MoN columns are also dense near the MoN/Mo interface. However, as the MoN layer grows, the columns start to regroup into large clusters, and voids start to appear between the clusters. Therefore, some strain relaxation may occur as the MoN columns attempt to fill the voids.

In the MoN layer of the as-deposited film, the FWHM of the diffraction peak is independent of the film depth [Fig. 3(b)]. This relationship implies that strain in the MoN layer is uniform at different depths since uniform strain does not change the peak width.[8] For the Mo layer, the FWHM of the diffraction peak is larger at the Mo/Si interface than at the MoN/Mo interface. This difference implies that the Mo grain size is smaller and/or the grains are more defective near the Si interface than near the MoN/Mo interface. After annealing, the FWHM of the MoN layer was observed to decrease, accompanied by a significant relief of the residual strain [Fig. 3(a)]. In comparison, an increase in the FWHM of the Mo layer accompanied a slight relief of the strain. Note that the melting temperatures of MoN and Mo are 1750 and 2623 °C, respectively.[12] These temperatures indicate that the annealing temperature (500 °C) is probably not high enough to initiate recrystallization or grain growth. Therefore, the decrease in the FWHM of the MoN layer could be caused by the reduction of defects, which may include crystallite defects, trapped gas ions and molecules, and voids. For the Mo layer, the increase in the FWHM after annealing probably means an increase in the defect concentration near the MoN/Mo interface. From these analyses, we conclude that annealing relieves strain and alters defect concentrations in the MoN and Mo layers.

Since the microstructure of films is sensitive to defects in general, annealing-induced changes in defect concentration might be expected to change the microstructure. This hypothesis was confirmed by examining the SEM micrographs of the MoN film before and after annealing. In the as-deposited film [Fig. 4(a)], there are large clusters with diameters of a few hundred nanometers, and the boundary around these clusters can be clearly seen. Each cluster consists of many very small columns (Fig. 1). After annealing [Fig. 4(b)], the microstructure changed significantly: the boundary between clusters was no longer well defined, and the grains in the clusters could be seen clearly. Therefore, annealing significantly changed the microstructure of the MoN layer, as is consistent with the observed large relief of strain in the annealed MoN layer.

In conclusion, we have applied cross-sectional x-ray microdiffraction to study depth-resolved residual strain in magnetron-sputtered MoN/Mo bilayer films. The MoN and Mo layers in the as-deposited film were found to be under in-plane compression, with large strain gradients as a function of depth. The observed strain profiles were explained in terms of atomic peening and void-induced strain relaxation. Annealing of the film causes significant strain relief and defect reduction in the MoN layer. In contrast, residual strain in the Mo layer is only slightly relieved, and the defect concentration increases after annealing. This study provides insights into the annealing effect on the depth-dependent structure and property of magnetron-sputtered nanocrystalline MoN/Mo films.

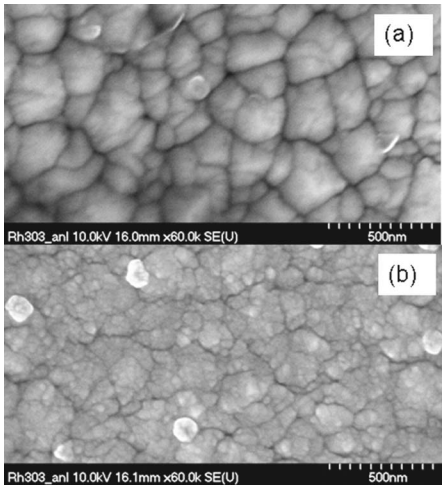

FIG. 4. Scanning electron micrographs of the surface of the MoN layer before (a) and after (b) annealing at 500 °C for 1 h.

The authors would like to thank S. Jiang, J. Tischler, and W. Yang for helping with the experiments and A. Erdemir for discussion. Use of the Advanced Photon Source was supported by the U.S. Department of Energy (DOE), Office of Science, Office of Basic Energy Sciences, under Contract No. W-31-109-Eng-38. The work at Argonne National Laboratory was supported by the DOE FreedomCAR and Vehicle Technologies Program. The work at Oak Ridge National Laboratory was supported by the DOE Office of Science, Division of Materials Sciences.

[1] D. B. Fenner, J. K. Hirvonen, and J. D. Demaree, in *Engineering Thin Films and Nanostructures with Ion Beams*, edited by Emile Knystautas (Taylor & Francis, Boca Raton, FL, 2005), Vol. 92, Chap. 4, pp. 117–228.
[2] V. Hauk, *Structure and Residual Stress Analysis by Nondestructive Methods* (Elsevier, Amsterdam, 1997), Chap. 2, pp. 132–215.
[3] P. Goudeau, P. Villain, N. Tamura, and H. A. Padmore, Appl. Phys. Lett. **83**, 51 (2003).
[4] G. C. A. M. Janssen and J. D. Kamminga, Appl. Phys. Lett. **85**, 3086 (2004).
[5] M. Ferrari and L. Lutterotti, J. Appl. Phys. **76**, 7246 (1994).
[6] C. Genzel, M. Broda, D. Dantz, and W. Reimers, J. Appl. Crystallogr. **32**, 779 (1999).
[7] G. E. Ice, B. C. Larson, W. Yang, J. D. Budai, J. Z. Tischler, J. W. L. Pang, R. I. Barabash, and W. Liu, J. Synchrotron Radiat. **12**, 155 (2005).
[8] B. D. Cullity and S. R. Stock, *Elements of X-ray Diffraction*, 3rd ed. (Prentice-Hall, Upper Saddle River, NJ, 2001), pp. 170–176.
[9] A. Misra and M. Nastasi, in *Engineering Thin Films and Nanostructures with Ion Beams*, edited by Emile Knystautas (Taylor & Francis, Boca Raton, FL, 2005), Vol. 92, Chap. 7, pp. 325–392.
[10] H. Windischmann, Crit. Rev. Solid State Mater. Sci. **17**, 547 (1992).
[11] A. Ezeilo, in *Analysis of Residual Stresses by Diffraction using Neutron and Synchrotron Radiation*, edited by M. E. Fitzpatrick and A. Lodini (Taylor & Francis, London, 2003), p. 260.
[12] *CRC Handbook of Chemistry and Physics*, 78th ed., edited by D. R. Lide (CRC, Boca Raton, FL, 1997), pp. 4–71.

Downloaded 06 Sep 2009 to 160.91.157.167. Redistribution subject to AIP license or copyright; see http://apl.aip.org/apl/copyright.jsp